

RESEARCH ARTICLE

Effect of solvent on properties of ZIF-8 and epoxy coating performance

Do Minh Thanh^{1,2} | Nguyen Ngoc Linh³ | Nguyen Thi Van Anh² | Nguyen Anh Hiep¹ |
Do Truc Vy¹ | Nguyen Thien Vuong¹ | Dao Phi Hung¹

¹Institute of Materials Science, Vietnam Academy of Science and Technology, Nghia Do, Hanoi, Vietnam

²Graduate University of Science and Technology, Vietnam Academy of Science and Technology, Nghia Do, Hanoi, Vietnam

³Institute of Medicine and Pharmacy, Thanh Do University, Hoai Duc, Hanoi, Vietnam

Correspondence

Dao Phi Hung, Institute of Materials Science, Vietnam Academy of Science and Technology, 18, Hoang Quoc Viet, Nghia Do, Hanoi, Vietnam.
Email: dphung@ims.vast.vn

Abstract

The effect of solvent, that is water or ethanol, on the properties of zeolitic imidazolate frameworks (ZIF)-8 materials, as well as the properties of epoxy coating filled with ZIF-8 materials, has been studied. The obtained results indicate that ZIF-8 materials synthesized in different solvents exhibit the sodalite phase and good crystallinity. However, there were slight differences in the *d*-spacing (between crystal planes) among ZIF-8 materials synthesized in different solvents, reflecting minor distortions in the crystal lattice or small variations in particle size or shape. Consequently, the ZIF-8 material synthesized in ethanol has a cubic morphology with a size of ≈ 100 nm, while the ZIF-8 material synthesized in water exhibits a thin-sheet morphology. The ZIF-8 materials improve the mechanical properties of epoxy coatings as well as their anticorrosion protection properties. The polarization curve shows that ZIF-8 materials shift the positive potential of epoxy coatings filled with ZIF-8 materials in comparison with neat epoxy coating. It means that the epoxy coating filled with ZIF-8 materials exhibits an inhibitory effect on the corrosion process of steel.

KEYWORDS

anticorrosion, epoxy coating, inhibitory effect, metal-organic frameworks, zeolitic imidazolate frameworks

1 | INTRODUCTION

According to the report by the National Association of Corrosion Engineers (NACE), the annual global cost of metal corrosion amounts to \$2.5 trillion (equivalent to 3.4% of the global gross domestic product [GDP] in 2016).¹ In addition to economic losses, undetected metal corrosion can lead to catastrophic events such as workplace accidents, equipment failure, and production disruptions. However, 15%–35% of corrosion-related losses (equivalent to \$375–875 billion) could be prevented with appropriate protection methods. Various approaches can be employed to mitigate metal corrosion. Among these, protection using protective coatings is highly effective and widely used. Epoxy resin-based coatings are commonly used as protective coatings against metal corrosion. Research findings have

demonstrated that epoxy resin-based coatings are significantly effective in protecting and extending the lifespan of metal products in various applications.² During use, corrosive agents can infiltrate and diffuse through the coating via micro-defects, leading to a reduction in the coating's properties. To prolong the service life of epoxy coatings and diversify their applications to meet practical demands, these coatings continue to attract significant interest from scientists and manufacturers. Metal-organic frameworks (MOFs) are a type of porous nanomaterial composed of metal ions and organic linkers.³ MOFs are utilized in various fields, including catalysis,⁴ energy storage and conversion,⁵ drug delivery,⁶ and sensing,⁷ owing to their high porosity, tunable pore morphology and size, diverse surface sites, and varied compositions.³ In the coatings field, MOFs can serve as corrosion inhibitors for certain metal substrates

due to their large surface area and abundance of functional groups, which facilitate their adsorption onto metal surfaces.⁸ Unlike traditional nanomaterial additives that only passively prevent the diffusion of corrosive agents from the environment into the organic coating, MOFs can be employed to develop adaptive anti-corrosion materials capable of countering various corrosion-inducing factors.⁹

Among MOFs materials, zeolitic imidazolate frameworks (ZIFs) have garnered significant attention and research interest from scientists. ZIFs are a type of MOFs with a zeolite-like geometry, featuring transition metal ions such as Fe, Co, Cu, and Zn as network nodes, coordinated with imidazole and its derivatives as linkers. Due to their high porosity, thermal stability, and chemical resistance, ZIFs are being investigated and applied in various fields, including electrochemical sensors,⁷ carbon capture, drug delivery, gas separation, catalysis, and protective anti-corrosion coatings.¹⁰ ZIFs can be synthesized using various methods, such as hydrothermal synthesis, microwave-assisted synthesis, or ultrasonic-assisted synthesis. Different approaches, including using surfactants, adjusting the metal ion-to-ligand ratio, or selecting specific solvents, can be employed to control the size and morphology of ZIFs.¹⁰ Tezerjani and colleagues investigated the effects of solvents and synthesis methods on the morphology of ZIF-8. They synthesized ZIF-8 using three methods: mixing, hydrothermal synthesis, and ultrasonic-assisted synthesis, in three main solvents: water, methanol (MeOH), and dimethylformamide (DMF). The results showed that ZIF-8 tends to form a cubic shape in MeOH, a rhombic dodecahedron shape in DMF, and a sheet-like morphology in water.¹¹

Zhang and colleagues studied the influence of the 2-methylimidazole/ Zn^{2+} molar ratio on some characteristics and properties of ZIF-8.¹² ZIF-8 was synthesized by mixing two solutions of Zn^{2+} and 2-methylimidazole in MeOH at room temperature. The results indicated that increasing the 2-methylimidazole/ Zn^{2+} mol ratio from 1 to 8 enhanced the synthesis yield from 25% to 51%, while the crystallinity of ZIF-8 also increased from 73% to 100%. However, further increases in this mol ratio led to decreases in both yield and crystallinity. According to Tsai and colleagues,¹³ the crystal size of ZIF-8 depends on the synthesis temperature. They synthesized ZIF-8 by mixing solutions containing Zn^{2+} salts and imidazole in MeOH at different temperatures ($-15\text{ }^{\circ}\text{C}$ to $60\text{ }^{\circ}\text{C}$). Their findings revealed that as the temperature increased from $-15\text{ }^{\circ}\text{C}$ to $60\text{ }^{\circ}\text{C}$, the average size of ZIF-8 crystals decreased from 78 to 26 nm, while the specific surface area increased from 220 to $336\text{ m}^2\text{ g}^{-1}$.

Based on the analysis above, it can be concluded that the solvent affects the morphology of ZIF-8, consequently, influences the properties of epoxy coatings containing ZIF-8 materials. In the current trend of increasing demand for environmentally friendly materials, this paper explores the impact of environmentally friendly solvents, namely water

TABLE 1 The composition of ZIF-8 materials.

No.	Zn(CH ₃ COO) ₂ (g)	2-Methylimidazole (g)	C ₂ H ₅ OH (mL)	H ₂ O (mL)	Code
1	0.1102	0.1864	20	–	Z14C
2	0.1112	0.1631	–	20	Z14H

and ethanol, on the properties of ZIF-8 materials and the epoxy coatings containing ZIF-8.

2 | MATERIALS AND METHODS

2.1 | Materials

Zinc acetate dihydrate and 2-methylimidazole, with a purity of $\geq 98\%$, were supplied by Sigma-Aldrich.

Water-based epoxy resin (trade name of GELR128), with a viscosity of 11 000–15 000 mPa s ($25\text{ }^{\circ}\text{C}$) and an epoxy equivalent weight of 184–190 (g eq⁻¹), was supplied by Epoxy Base Electronic Material Corporation Limited (China).

Water-based curing agent (trade name of Kingcure X-980 W), based on modified polyamine, with a viscosity of 10 000–15 000 mPa s ($25\text{ }^{\circ}\text{C}$), an amine value of 210 ± 15 , a density of 1.13 g mL^{-1} ($25\text{ }^{\circ}\text{C}$), and solid content of $80 \pm 3\%$, was provided by Sanho Chemical Co., Ltd. (Taiwan).

Other chemicals, such as absolute ethanol (China) and distilled water.

2.2 | ZIF-8 preparation

The ZIF-8 materials were prepared using the following procedure:

- i. Preparation of Zn^{2+} solution: Zinc acetate dihydrate was dissolved in water or ethanol by stirring on a magnetic stirrer, followed by ultrasonication for 10 min to obtain a homogeneous solution.
- ii. Preparation of 2-methylimidazole solution: 2-Methylimidazole was dissolved for 10 min in a separate portion of ethanol.
- iii. Mixing solutions: The 2-methylimidazole solution was gradually added to the Zn^{2+} solution under gentle stirring. Under these conditions, the reaction occurred and ZIF-8 particles gradually formed.

iv. Recovery and purification of the product: After 24 h of reaction, ZIF-8 was collected by centrifugation at 12 000 rpm (Nuve NF1200 centrifuge). The product was washed five times with ethanol to remove impurities and residual components, and then dried at $50\text{ }^{\circ}\text{C}$ in a vacuum oven.

The composition used for the preparation of ZIF-8 is presented in Table 1.

TABLE 2 The composition of epoxy nanocomposite coating containing ZIF-8.

No.	Code Chemicals	Ep	EpZ14C	EpZ14H
1	Epoxy (g)	5	5	5
2	Z14C (g)	–	0.02	–
3	Z14H (g)	–	–	0.02
4	H ₂ O (g)	–	2	2
5	Curing agent (g)	5	5	5

2.3 | Epoxy coating filled with ZIF-8 preparation

The water-based epoxy coating was prepared through the following steps:

First, ZIF-8 nanoparticles were dispersed in water at a mass ratio of 1:10 using a magnetic stirrer and ultrasonicated with a Branson Sonifier 450 for 15 min. The resulting suspension was then blended with the hardener Kingcure X-980 W using a laboratory ball mill for 24 h. Then, the obtained mixture of the hardener and ZIF-8 was subsequently combined with the epoxy resin and applied to clean steel and glass plates using a film applicator (Erichsen model 306) to achieve a wet film thickness of 120 μm . The coatings were allowed to cure for 7 days under ambient conditions and then stabilized at 25 °C and 50% relative humidity for at least 24 h prior to further testing. The composition of the ZIF-8 nanocomposite coating is summarized in Table 2.

The samples for natural salt spray testing were prepared by coating both sides of CT 45 steel substrates with the investigated nanocomposite coating. The edges of the samples were then sealed, and the samples were cut in an X shape and allowed to stabilize for at least 7 days prior to testing.

The samples for electrochemical measurements were prepared by applying the investigated nanocomposite coating onto CT 45 steel substrates. The coated surfaces were then mounted on PVC tubes (42 mm in diameter and 15 cm in height). The samples were allowed to stabilize for 7 days before 3% NaCl solution was applied.

2.4 | Analysis

2.4.1 | Infrared spectroscopy analysis

The functional groups of ZIF-8 materials before and after organic modification were identified using Fourier-transform infrared spectroscopy (FT-IR) in transmission mode on a Nicolet iS10 spectrometer (Thermo Scientific, USA). The ZIF-8 materials were mixed with KBr powder at a 1:50 mass ratio and pressed into pellets for analysis.

2.4.2 | Morphological characterization

The morphology of the nanoparticles before and after organic modification was examined using field emission scanning electron microscopy (FESEM) images recorded on a Hitachi S-4800 instrument (Japan). To enhance conductivity, the samples were coated with a thin layer of platinum.

2.4.3 | X-ray diffraction patterns

The phase characteristics and crystallinity of the material were determined by X-ray diffraction (XRD) analysis. The XRD patterns were recorded at room temperature using $\text{CuK}\alpha$ ($\lambda = 1.5406 \text{ \AA}$) with a scanning speed of 0.01° per second on a D8-Advance 5005 diffractometer.

2.4.4 | Determination of mechanical properties of coating

Several mechanical properties of the nanocomposite coating were evaluated, including pendulum hardness using an Erichsen hardness tester (model 299/300) (TCVN 2098:2007), impact resistance measured with the Erichsen 304 ISO device (TCVN 2100-1:2013), and adhesion strength to the steel substrate using the Elcometer F510 (model T) (ISO 4624). Each test was performed in triplicate, and the average value was reported.

2.4.5 | Corrosion resistance testing

The corrosion protection performance of the epoxy coating was tested using a neutral salt spray test performed in the Q-Fog CCT 600 chamber, following ASTM B117 standard. The polarization curves of the epoxy coatings immersed in a 3 wt% NaCl solution were recorded using the Metrohm DropSens device (Spain) at a scan rate of 1 mV s^{-1} . A three-electrode system was employed, where a saturated calomel electrode served as the reference electrode, the C45 steel coated with the investigated coatings (exposure area: 13.847 cm^2) acted as the working electrode, and graphite was used as the counter electrode.

3 | RESULTS AND DISCUSSION

3.1 | Infrared spectroscopy analysis of ZIF-8 materials

The infrared spectra of Z14C and Z14H are presented in Figure 1. As shown in Figure 1, the infrared spectra of Z14C and Z14H exhibit similar patterns with characteristic peaks corresponding to the bonds in 2-methylimidazole. For instance, the peak at 3115 cm^{-1} is characteristic of

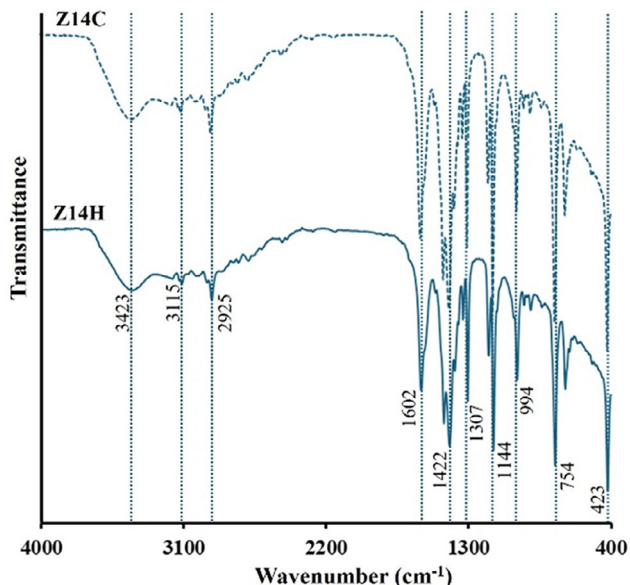


FIGURE 1 The infrared spectra of ZIF-8 synthesized in water or ethanol.

the stretching vibration of the aromatic C—H bond, while the peaks at 2925 and 1307 cm^{-1} correspond to the stretching and bending vibrations of the C—H bond in the $-\text{CH}_3$ group, respectively. The peak at 1602 cm^{-1} is associated with the stretching vibration of the C=N double bond, while the peaks at 1144 and 994 cm^{-1} are attributed to the stretching and deformation vibrations of the C—N bond in the imidazole ring.¹⁴ Additionally, the peak at 423 cm^{-1} corresponds to the stretching vibration of the Zn—N bond between the Zn^{2+} ion and the 2-methylimidazolate ligand,¹¹ confirming the successful synthesis of ZIF-8.

3.2 | X-ray diffraction patterns

The X-ray diffraction (XRD) patterns of ZIF-8 synthesized in water (Z14H) and ethanol (Z14C) are presented in Figures 2 and 3, respectively.

Observing Figures 2 and 3, the XRD patterns of Z14H and Z14C show identical diffraction peaks at 2θ angles of 7.26°, 10.41°, 12.63°, 15.48°, 18.03°, 22.14°, 26.64°, and 29.75°, corresponding to (0 1 1), (0 2 2), (1 1 2), (0 1 3), (2 2 2), (1 1 4), (2 2 3), and (3 3 4) crystal planes. These peaks are consistent with the cubic crystal structure (sodalite—SOD) of ZIF-8.^{11,14} No diffraction peaks corresponding to ZnO are observed. Moreover, the diffraction peaks of both Z14H and Z14C are clear and sharp, demonstrating that ZIF-8 synthesized in either water or ethanol has good crystallinity. Comparing the XRD patterns, Z14H exhibits diffraction peaks similar to those of Z14C, but there are slight differences in the d -spacing (between crystal planes) and the intensity of the peaks. The minor shifts in d -spacing might

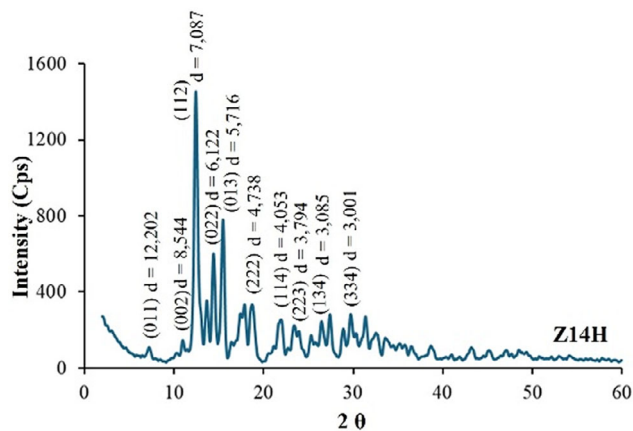


FIGURE 2 X-ray diffraction (XRD) pattern of ZIF-8 synthesized in water.

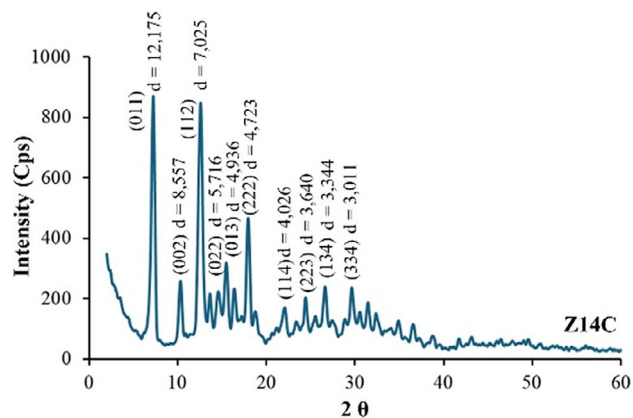


FIGURE 3 X-ray diffraction (XRD) pattern of ZIF-8 synthesized in ethanol.

reflect small distortions in the crystal lattice or variations in particle size or morphology.

3.3 | Morphology analysis

FESEM images at different magnifications of ZIF-8 synthesized with a $\text{Zn}^{2+}/2$ -methylimidazole molar ratio of 1:4 in water or ethanol are presented in Figure 4.

As shown in Figure 4, it can be observed that ZIF-8 particles synthesized in ethanol exhibit a cubic morphology with an average size of approximately ≈ 100 nm, and the particles are relatively uniform. In contrast, ZIF-8 particles synthesized in water display a thin-sheet morphology. These differences in polymorphic forms are attributed to the synthesis conditions. Although both forms possess a cubic crystal structure, the polymorphic variation of ZIF-8 synthesized in water and ethanol results in slight distortions in the interplanar spacing (d).

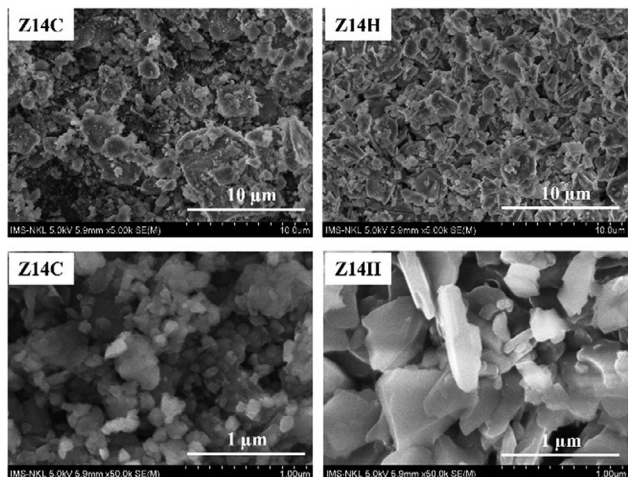


FIGURE 4 FESEM images of ZIF-8 materials synthesized in water or ethanol.

TABLE 3 Some mechanical properties of epoxy coatings filled with ZIF-8 materials synthesized in water and ethanol.

Sample	Pendulum hardness	Impact resistance (kG.cm)	Adhesion (MPa)
Ep	197.67	96	0.95
EpZ14H	211.67	122	1.02
EpZ14C	220.67	112	1.03

3.4 | Effect of ZIF-8 materials synthesized in water or ethanol on epoxy coating’s mechanical properties

The effect of ZIF-8 synthesized in water and ethanol on the mechanical properties of epoxy coatings containing 2 wt% ZIF-8 is presented in Table 3.

From Table 3, it can be seen that ZIF-8 enhances the mechanical properties of the epoxy coating, such as hardness, impact resistance, and adhesion. However, the extent of improvement varies depending on the solvent used for ZIF-8 synthesis. ZIF-8 synthesized in water primarily enhances impact resistance, whereas ZIF-8 synthesized in ethanol improves hardness, with only minor differences in adhesion observed between the coatings containing the two types of ZIF-8.

This phenomenon can be explained by the differences in particle morphology. ZIF-8 synthesized in ethanol exhibits a cubic shape with a relatively small particle size (≈ 100 nm). Owing to their uniform geometry and compact structure, these cubic particles are more evenly dispersed within the polymer matrix, which facilitates efficient stress transfer and enhances the mechanical strength of the coating, thereby improving properties such as pendulum hardness and impact resistance. In contrast, ZIF-8 synthesized in water shows a sheet-like morphology that provides a larger surface area, promoting stronger interaction with the poly-

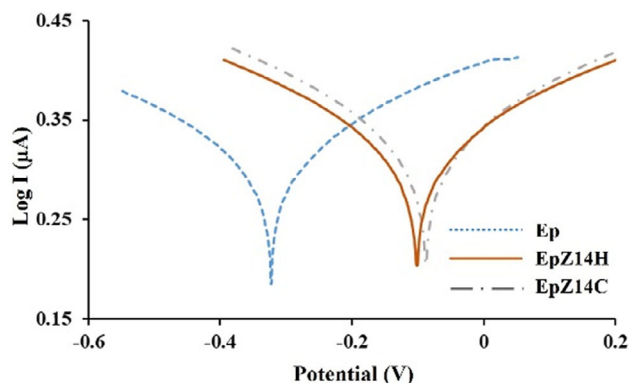


FIGURE 5 Polarization curve of epoxy coating filled with ZIF-8 after 6 days immersion in 3 wt% NaCl solution.

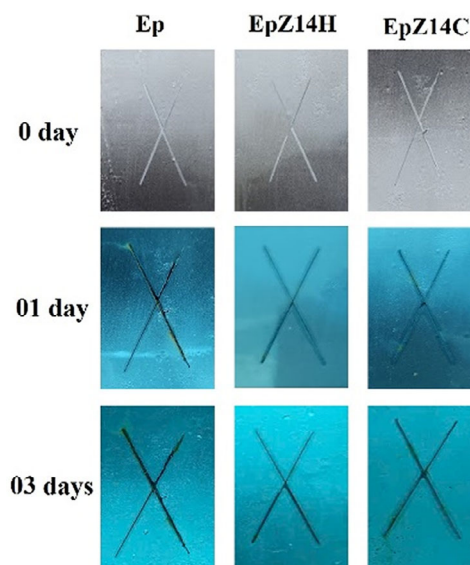


FIGURE 6 Images of investigated samples upon natural salt spray test.

mer matrix and thus contributing to improve the coating durability.

3.5 | Effect of ZIF-8 materials synthesized in water or ethanol on epoxy coating’s anticorrosion properties

The effect of the solvent used for ZIF-8 synthesis on the corrosion protection performance of the epoxy coating containing ZIF-8 was evaluated by polarization measurement and neutral salt spray tests. The polarization curves and images of the neutral salt spray test for the epoxy coatings with different formulations are presented in Figures 5 and 6, respectively, while the electrochemical parameters of the coatings are summarized in Table 4.

From Figure 5 and Table 4, it can be seen that when ZIF-8 is added to the coating, the corrosion potential of the

TABLE 4 The parameters of the epoxy coatings without ZIF-8 (Ep) and with ZIF-8 after 6 days of immersion in 3% NaCl solution.

Samples	E_{corr} (mV)	I_{corr} (μA)
Ep	-323	2.11
EpZ14H	-100	2.02
EpZ14C	-89	2.06

epoxy coating leads to a positive shift. The original epoxy coating has a corrosion potential (E_{corr}) of -323 mV, while the coating containing ZIF-8 has a corrosion potential of approximately $E_{\text{corr}} \approx -100$ mV. This result indicates that the steel substrate is less susceptible to oxidation (reduced corrosion). The improvement may be attributed to the ability of ZIF-8 to gradually release 2-methylimidazole under environmental conditions, which act as a corrosion inhibitor for steel.¹⁵ Consequently, the presence of ZIF-8 enhances the corrosion protection performance of epoxy coating. Furthermore, Table 4 reveals that the corrosion current density of the coatings follows the order: Ep > EpZ14C > EpZ14H. This trend indicates that the corrosion protection capability of the epoxy coating containing ZIF-8 synthesized in water is the best among the examined coatings.

To evaluate the corrosion protection ability of the epoxy coating with and without ZIF-8, neutral salt spray testing was conducted. Images of the test samples during the neutral salt spray process are shown in Figure 6. Observation of Figure 6 reveals that the scratch on the sample of the epoxy coating without ZIF-8 shows signs of corrosion after just 24 h of salt spray exposure. In contrast, for the epoxy coating containing ZIF-8, the scratch remains unaffected after 24 h of salt spray exposure. After 72 h of neutral salt spray, the steel sample coated with epoxy containing ZIF-8 synthesized in ethanol shows more noticeable signs of corrosion compared to the sample coated with epoxy containing ZIF-8 synthesized in water. It can be observed that the corrosion protection ability of the coating containing ZIF-8 synthesized in water is better than that of the coating containing ZIF-8 synthesized in ethanol. Although both ZIF-8 samples were synthesized in ethanol and water, they both have a cubic crystal structure. However, due to the synthesis conditions, a slight distortion in the crystal lattice occurred. While ZIF-8 synthesized in ethanol maintains its cubic shape with a small particle size (≈ 100 nm), ZIF-8 synthesized in water takes on a sheet-like form. The distortion in the crystal lattice affects the stability of ZIF-8. Under environmental conditions, ZIF-8 will release 2-methylimidazole, which has the ability to inhibit steel corrosion. If the ZIF-8 material is less stable, it will have better corrosion protection capability. Furthermore, the better corrosion resistance of epoxy coatings containing water-derived ZIF-8 compared with ethanol-derived ZIF-8 can be mechanistically explained by the interplay of morphology and structural stability. The sheet-like ZIF-8 particles synthesized in water provide a larger surface area and more extended interfaces with the epoxy matrix, improving the

physical barrier effect against chloride ion ingress. In addition, the slight lattice distortion observed in water-derived ZIF-8 reduces its crystallographic stability, facilitating the gradual release of 2-methylimidazole molecules under corrosive conditions. These molecules act as active corrosion inhibitors, adsorbing on the steel surface and mitigating anodic and cathodic reactions. By contrast, ethanol-derived ZIF-8 with cubic morphology exhibits higher structural integrity, which slows the release of 2-methylimidazole and limits active inhibition, despite its positive contribution to coating hardness. Thus, the superior corrosion protection of water-synthesized ZIF-8 arises from the synergistic effect of a larger barrier surface area and more efficient inhibitor release.

The above results confirm that solvent selection not only influences the morphology and crystallinity of ZIF-8 but also directly affects the performance of epoxy coatings. Compared to prior works focusing on methanol or DMF,^{11–13} our study highlights the novelty of employing green solvents. Tezerjani *et al.*¹¹ reported cubic and rhombic dodecahedral ZIF-8 crystals in MeOH and DMF, whereas our study demonstrates that ethanol produces highly uniform cubic nanoparticles (≈ 100 nm), and water yields sheet-like particles. Beyond structural characterization, our findings provide new insights by systematically linking solvent-dependent ZIF-8 properties to functional performance. Ethanol-derived ZIF-8 improves hardness, while water-derived ZIF-8 enhances impact resistance and delivers superior corrosion protection, with E_{corr} shifting positively from -323 mV to ≈ -100 mV. This emphasizes that green solvents not only ensure sustainability but also offer a practical strategy to tailor coating properties.

4 | CONCLUSION

ZIF-8 materials synthesized in different solvents exhibit the sodalite phase and good crystallinity. However, there were slight differences in the d -spacing (between crystal planes) among ZIF-8 materials synthesized in different solvents, reflecting minor distortions in the crystal lattice or small variations in particle size or shape. Consequently, the ZIF-8 material synthesized in ethanol has a cubic morphology with a size of ≈ 100 nm, while the ZIF-8 material synthesized in water exhibits a thin-sheet morphology. The ZIF-8 materials improve the mechanical properties of epoxy coatings as well as their anticorrosion protection properties. The polarization curve indicates that epoxy coatings filled with ZIF-8 materials exhibit an inhibitory effect on the corrosion process of steel.

ACKNOWLEDGMENTS

This work received support from the Annual Financial Fund of the Vietnam Academy of Science and Technology.

CONFLICT OF INTEREST STATEMENT

The authors declare no conflicts of interest.

REFERENCES

1. G. Koch, J. Varney, N. Thompson, O. Moghissi, M. Gould, J. Payer. *International Measures of Prevention, Application, and Economics of Corrosion Technologies Study—NACE International*, NACE International, Houston, TX **2016**. <http://impact.nace.org/documents/Nace-International-Report.pdf>
2. T. D. Nguyen, T. T. Thai, Q. T. Do, T. M. Tran, T. T. T. Nguyen, G. V. Pham, A. S. Nguyen. Preparation and characterization of waterborne epoxy coatings containing conductive PANi/silica nanoparticles, *Vietnam J. Chem.* **2020**, *58*, 206–2011.
3. T. P. Nguyen, T. H. Do, T. Doneux, H. N. Nguyen, T. M. T. Dinh. Synthesis of metal organic framework based on Cu and benzene-1,3,5-tricarboxylic acid (H3BTC) by potentiodynamic method for CO₂ adsorption, *Vietnam J. Chem.* **2023**, *61*, 210–219.
4. A. Bavykina, N. Kolobov, I. S. Khan, J. A. Bau, A. Ramirez, J. Gascon. Metal-organic frameworks in heterogeneous catalysis: Recent progress, new trends, and future perspectives, *Chem. Rev.* **2020**, *120*, 8468–8535. <https://doi.org/10.1021/acs.chemrev.9b00685>
5. H. Wang, Q. L. Zhu, R. Zou, Q. Xu. Review: Metal-organic frameworks for energy applications, *Chem* **2017**, *2*, 52–80. <https://doi.org/10.1016/j.chempr.2016.12.002>
6. H. D. Lawson, S. P. Walton, C. Chan. Metal-organic frameworks for drug delivery: A design perspective, *ACS Appl. Mater. Interfaces* **2021**, *13*, 7004–7020. <https://doi.org/10.1021/acsami.1c01089>
7. P. Kukkar, K. H. Kim, D. Kukkar, P. Singh. Review: Recent advances in the synthesis techniques for zeolitic imidazolate frameworks and their sensing applications, *Coord. Chem. Rev.* **2021**, *446*, 214109. <https://doi.org/10.1016/j.ccr.2021.214109>
8. P. Silva, S. M. Vilela, J. P. Tome, F. A. Almeida Paz. Multifunctional metal-organic frameworks: from academia to industrial applications, *Chem. Soc. Rev.* **2015**, *44*, 6774–6803. <https://doi.org/10.1039/C5CS00307E>
9. X. Li, Y. Di, Z. Chen, W. Yang. pH-responsive bimetallic Ce-ZIF-8 nanocontainer for the active corrosion protection of Al alloys, *Colloids Surf. A: Physicochem. Eng. Asp.* **2022**, *653*, 129990. <https://doi.org/10.1016/j.colsurfa.2022.129990>
10. S. Kouser, A. Hezam, M. J. N. Khadri, S. A. Khanum. A review on zeolite imidazole frameworks: Synthesis, properties, and applications, *J. Porous Mater.* **2022**, *29*, 663–681. <https://doi.org/10.1007/s10934-021-01184-z>
11. A. A. Tezerjani, R. Halladj, S. Askari. Different view of solvent effect on the synthesis methods of zeolitic imidazolate framework-8 to tuning the crystal structure and properties, *RSC Adv.* **2021**, *11*, 19914. <https://doi.org/10.1039/D1RA02856A>
12. Y. Zhang, Y. Jia, M. Li, L. Hou. Influence of the 2-methylimidazole/zinc nitrate hexahydrate molar ratio on the synthesis of zeolitic imidazolate framework-8 crystals at room temperature, *Sci. Rep.* **2018**, *8*, 9597. <https://doi.org/10.1038/s41598-018-28015-7>
13. C. W. Tsai, E. H. G. Langner. The effect of synthesis temperature on the particle size of nano-ZIF-8, *Micropor. Mesopor. Mater.* **2016**, *221*, 8–13. <https://doi.org/10.1016/j.micromeso.2015.08.041>
14. B. Hachuła, M. Nowak, J. Kusz. Crystal and molecular structure analysis of 2-methylimidazole, *J. Chem. Crystallogr.* **2010**, *40*, 201–206.
15. S. Elavanrasan, K. Kannan, V. Chandrasekaran. 2-methyl imidazole as a corrosion inhibitor for mild steel in acid medium, *Asian J. Chem.* **2006**, *18*, 2637–2644.

How to cite this article: D. M. Thanh, N. N. Linh, N. T. Van Anh, N. A. Hiep, D. T. Vy, N. T. Vuong, D. P. Hung, Effect of solvent on properties of ZIF-8 and epoxy coating performance, *Vietnam J. Chem.* **2025**, *1*. <https://doi.org/10.1002/vjch.70088>